International Journal of Hydrogen Energy 52 (2024) 761–774

Contents lists available at ScienceDirect

International Journal of Hydrogen Energy

journal homepage: www.elsevier.com/locate/he

Spatially-explicit optimization of an integrated wind-hydrogen supply chain network for the transport sector: The case study of Sicily

E. Cutore [a], A. Fichera [a], G. Inturri [a], M. Le Pira [b], R. Volpe [a,*]

[a] Department of Electrical, Electronic, and Computer Engineering, University of Catania, Italy
[b] Department of Civil Engineering and Architecture, University of Catania, Italy

ARTICLE INFO

Keywords:
Renewable hydrogen
Design
Operation and management
MILP
Bus and railway
Supply chain network

ABSTRACT

Almost half of the European railways are served by diesel-powered trains used for both cargo and passenger transport. Similar considerations apply to the bus sector in urban and suburban areas. The decarbonization of the transport sector can be achieved by using hydrogen as a fuel for trains and buses. However, the main barrier to adopting hydrogen fuel cell trains and buses is the construction of adequate infrastructure. Thus, to foster a sustainable energy transition, existing renewable plants should be considered when designing new hydrogen supply chains. In the proposed Sicilian case study, existing wind farms are chosen as electricity production plants. Most of them have been shut down due to grid unbalancing issues; still, the curtailed renewable electricity could be used to produce zero-carbon hydrogen via water electrolysis, significantly reducing costs. To account for this opportunity, this study models the hydrogen production, transportation, and refueling stages, employing a mixed-integer linear programming approach to find the optimal location and capacities of hydrogen infrastructure, while minimizing the total daily cost of the supply chain. The model is applied to Sicily and different scenarios for varying hydrogen demands for trains and buses are analyzed and discussed. Results show that capital expenses cover more than 90% of the total cost of the supply chain, with a hydrogen cost dispensed at the filling station ranging from 6.32 to 9.02 €/kgH_2. The environmental analysis shows that as hydrogen demand rises, so do the carbon emissions from the distribution stage. However, the impact of using wind-generated electricity in terms of avoided emissions is notably greater. Finally, it is shown that transporting hydrogen in gaseous form using tube trailers is economically more attractive than transportation in liquid form with tanker trucks in the early stages of the network.

1. Introduction

It is widely accepted that hydrogen may have a pivotal role in pushing the transition to affordable and clean cities and communities [1]. For this transformation to take place, particular attention has to be devoted to hydrogen-based investments in hard-to-abate sectors, such as the transport sector, responsible for the 26% of European greenhouse gas emissions (GHGs) [2]. This is even more urgent if the difficulties arising during the pandemic period and the current geopolitical tensions are taken into consideration. The oil and gas markets are experiencing an unstable period, posing serious concerns for global economies, which heavily rely on oil and gas for electricity production [3]. As a counterpart, renewable sources, whose integration into the energy production and distribution systems is already well established, can significantly contribute to more intensive exploitation of hydrogen-based applications, especially for the aforementioned transport sector.

Nevertheless, the production of hydrogen from renewable sources poses several questions that require comprehensive analyses. Aspects related to the conversion, distribution, and refueling of hydrogen should also be coupled with the optimal selection of the renewable source as well as with spatial and temporal issues referring to the location of renewable plants and distribution routes – especially for public transport services, such as railway and buses – and with the annual production from renewables.

Under these premises, this paper offers a model tailored to the specific case study of Sicily, a region where hydrogen can be produced from existing wind farms, usually shut down due to grid congestion issues. Indeed, the valorization of electricity produced from wind paves the way for sustainable planning of hydrogen supply chain (HSC) networks. This

* *Corresponding author.*
E-mail address: rosaria.volpe@unict.it (R. Volpe).

https://doi.org/10.1016/j.ijhydene.2023.10.105
Received 23 January 2023; Received in revised form 6 October 2023; Accepted 9 October 2023
Available online 31 October 2023

Nomenclature

Acronyms

PNRR	Italian Recovery and Resilience Plan
NGEU	NextGenerationEU
IEA	International Energy Agency
H_2ICE	Hydrogen internal combustion engine
HSC	Hydrogen Supply Chain
FCMU	Fuel Cell Multiple Unit
FCEB	Fuel Cell-Electric Bus
GH_2	Gaseous Hydrogen
LH_2	Liquefied Hydrogen

Indexes

g, g' with g ≠ g'	Geographic location (subregion)
j	Size of a production facility
i	Physical form of hydrogen

Parameters

D_{H_2}	Daily hydrogen demand [kgH_2 /day]
FE	Fuel economy [kgH_2 /km]
HU	Number of hydrogen-powered units (FCMUs or FCEBs)
pcc_{ij}	Capital costs of a production facility of size j producing hydrogen in the physical form i [€]
upc_{ij}	Unit production cost for producing hydrogen in physical form i in a production facility of size j [€/ kgH_2]
$pcap_{ij}^{min}$	Minimum production capacity of a production facility of size j producing hydrogen in physical form i [kgH_2/ day]
$pcap_{ij}^{max}$	Maximum production capacity of a production facility of size j producing hydrogen in physical form i [kgH_2/ day]
$tucap_i^{max}$	Maximum delivery capacity of a transport unit transporting hydrogen in physical form i [kgH_2]
$speed_i$	Average speed of a transport unit transporting hydrogen in physical form i [km/hr]
$lutime_i$	Loading/Unloading time of a transport unit transporting hydrogen in physical form i [hr]
$driver_i$	Driver cost for a transport unit transporting hydrogen in physical form i [€/hr]
mc_i	Maintenance costs of a transport unit transporting hydrogen in physical form i [€/km]
fc_i	Fuel consumption of a transport unit transporting hydrogen in physical form i [km/l]
$tucc_i$	Capital cost of a transport unit transporting hydrogen in physical form i [€]
$fuel_i$	Fuel price for a transport unit transporting hydrogen in physical form i [€/l]
$flow_i^{max}$	Maximum flow rate of hydrogen for a transport unit transporting hydrogen in physical form i [kgH_2/day]
rcc_i	Capital costs of a hydrogen refueling station receiving hydrogen in physical form i [€]
$rcap_i^{max}$	Maximum daily capacity of hydrogen refueling station receiving hydrogen in physical form i [kgH_2/day]
$hdem_g$	Total demand of hydrogen at location g [kgH_2/day]
dist	daily average covered distance
$dist_{gg'}$	Euclidean distance between location g and g' [km]
res_g^{max}	Maximum production capacity of hydrogen from renewable energy sources at location g [kgH_2/day]
α	Hydrogen supply chain operating period [day/year]
ccf	Capital charge factor [year]

Continuous variables

$HF_{gg'i}$	Flow from location g to g' of hydrogen in physical form i [kgH_2/day]
HPR_{gij}	Production rate of a production facility of size j producing hydrogen in physical form i at location g [kgH_2/day]
$HDEM_{gi}$	Demand for hydrogen in physical form i at location g [kgH_2/day]
HSC	Hydrogen supply chain total daily cost [€/day]
FCC	Facilities capital costs [€]
POC	Production operating costs [€/day]
TCC	Transport capital costs [€]
TOC	Transport operating costs [€/day]
TMC	Transport maintenance cost [€/day]
TLC	Transport labor cost [€/day]
TFC	Transport fuel cost [€/day]

Binary variables

$Y_{gg'i}$	1 if a connection between location g and g' is established, 0 otherwise

Integer variables

NP_{gij}	Number of production facilities of size j producing hydrogen in physical form i at location g
$NTU_{gg'i}$	Number of transportation units transporting hydrogen in physical form i from location g to g'
NRS_{gi}	Number of refueling stations receiving hydrogen in physical form i at location g

approach allows investment costs for installing new facilities to be overcome by favoring the exploitation of existing infrastructures and auxiliary equipment. This model can serve as a valuable tool for stakeholders, assisting them in the decision-making process concerning the cost-effectiveness of new hydrogen supply chain infrastructure installation within the regional context. These facilities have the objective of bolstering the capacity for low-carbon hydrogen production, catering to different end-users, including regional passenger trains and urban buses.

1.1. European and Italian normative context for the transport sector

The utilization of hydrogen as an energy carrier is attracting interest and its exploitation for energy purposes is now intensively encouraged by current regulations and subsidies. Particularly within the transport sector, the Communication COM/2018/773 from the European Commission advised each Member State to take significant steps towards the diffusion of technologies such as electric batteries, fuel cells, and hydrogen internal combustion engines (H_2ICE) [4]. Following this, the measures contained in the package "*A hydrogen strategy for a climate-neutral Europe*" aims to achieve the ambitious goal of installing at least 40 GW of water electrolyzers by 2030, and attaining climate-neutrality by 2050 [5].

National hydrogen-related policies allocate a substantial amount of investment towards research and development activities to propel experimental efforts and numerical investigation in the field of innovative electrolyzers and HSC designs. In Italy, the National Recovery and Resilience Plan (PNRR), established under the *NextGenerationEU* (NGEU) program, dedicates a significant portion of funding to research centers and industries. Specifically, 30 million euros are earmarked for companies, and 20 million for research bodies and universities (Mission M2 "*Green revolution and ecological transition*", Component C2 "*Renewable energy, hydrogen, grid and sustainable mobility*"), to foster the development and construction of hydrogen production facilities, tailored specifically for the transport sector [6]. Furthermore, Component C2 of Mission M2 explicitly promotes the development of hydrogen-based mobility infrastructures, especially for the regional

railway networks. In these networks, Fuel Cell Multiple Units (FCMUs) are planned to replace diesel-powered trains where electrification is not economically sustainable – as is the case of the 40% of the entire Italian national railway, particularly in southern Italy [6]. Hydrogen-powered technologies offer a promising alternative to diesel combustion engines in rail transportation. Among various applications, FCMUs are at a more mature stage and exhibit potential to compete favorably with diesel-powered trains in the near future. This potential is particularly evident in scenarios where the economic feasibility of hydrogen production is high, such as harnessing excess energy from variable renewable sources. From an economic standpoint, FCMU technology surpasses catenary electrification in cases of low service frequencies [7]. It also overcomes the technical limitations of electric batteries by offering longer operating ranges and fast refueling capabilities, with downtimes of approximately 15 min, comparable to other solutions [8]. FCMUs can operate for more than 18 h continuously, making them economically advantageous, particularly for longer non-electrified routes exceeding 100 km [7]. Additionally, within the same mission of the PNRR, specific actions are allocated for sustainable transport infrastructure development, including metro systems, trams, and buses for both metropolitan and regional routes, with a particular focus on the South of Italy, which will receive a dedicated portion of 50% of the financial resources to facilitate the hydrogen transition within this market segment [6].

Similarly, fuel cell-electric buses (FCEBs) could prove to be more cost-efficient than their electric counterparts due to the following considerations: *i)* they offer operating ranges of up to 300 km (or 16 h) with a full tank, and *ii)* rapid refueling takes less than 20 min compared to over 1 h for a 100 % electric-based bus [9]. Short downtimes significantly streamline the logistics required to refuel entire bus fleets in shorter timeframes, *e.g.,* for example, overnight, particularly in cases where a high number of buses serve densely populated urban areas. Moreover, FCEBs provide all the advantages associated with an electric engine, including zero tailpipe emissions, low levels of noise, and enhanced passenger comfort due to reduced cabin vibrations.

Therefore, as also promoted by national regulations, hydrogen-powered trains and buses are poised to be effective alternatives to diesel- and electric-based trains and buses. This regulatory framework will not only contribute to the decarbonization of the transport sector, which is critically dependent on oil as the main energy carrier [10] but also to the enhancement of living standards and quality of life of citizens, with hydrogen being a flexible and potentially carbon-free technology [11]. Moreover, the need for an energy transition is further driven by the fact that, as stated by the International Energy Agency (IEA), the percentage of total passengers choosing trains and buses for their activities is projected to rise to 12.60% in the net-zero scenario envisaged by 2030 [12]. Consequently, the European regulatory scenario encourages the exploitation of hydrogen-powered trains, especially on long non-electrified routes where the investment costs for catenary electrification would be prohibitively high (estimated to be around 2.8 M€/ km [13]).

1.2. The modeling of hydrogen supply chains

This work explores the effective analysis of hydrogen penetration in the transport sector through the lens of Hydrogen Supply Chain (HSC) design. It entails studying the various stages of hydrogen supply, from production to vehicle refueling.

Supply chain management (SCM) is a branch of operations research that focuses on logistics and tackles the challenge of designing and managing a supply chain network to meet specific goals (economic, environmental, social, etc.) within given constraints. Numerous studies in the literature employ an optimization approach address supply chain network design issues, with mixed-integer linear programming often being the preferred method due to its ability to handle two distinct sets of decision variables [14]. The first set consists of design variables, which are integers (binary or discrete), and in this context, control the activation or deactivation of supply chain infrastructures across different locations (or nodes) and routes (or links). The second set comprises operation variables, which are continuous managing supply chain processes like production and flow rates.

Almansoori and Shah [15] pioneered a general-purpose model for the optimal design of an automotive supply chain, where the mathematical model was formulated as a MILP model aiming to minimize both the capital and operating costs of the HSC. A follow-up study extended this model to account for a multi-period optimization [16]. Wickham et al. dealt with the design of the HSC for the transport sector but focused on the optimization of the purification and separation stages, necessary to achieve the purity requirements for automotive applications [17]. Purification technologies are also modeled in the work of Yoon et al. [18], proposing a multi-period optimization of a hydrogen supply chain with by-product hydrogen and natural gas pipelines. Ehrenstein et al. brought attention to the importance of sustainability impact assessment of hydrogen supply chains in the passenger car sector [19]. In this paper, unlike other papers, the objective function is constructed to minimize the levels of planetary boundary transgression. Similarly, in another study the HSC is modeled to minimize the overall costs, while certain constraints have been posed to guarantee a lower impact on the environment [20]. Given the non-dispatchable nature of some energy sources and inevitable uncertainty in the demand profile of the final users, storage systems are included to overcome supply-demand mismatches over time. In this direction, Seo et al. proposed an optimization model explicitly accounting for hydrogen storage systems with the aim of determining whether these systems may be better utilized in a centralized or decentralized configuration [21]. From the achieved results, central hydrogen production and liquefaction units are the preferred options. Hydrogen supply chains cannot be viewed as isolated systems, particularly when considering the interchangeability of hydrogen and electricity. A recent study introduced a spatial optimization framework that combines geographical information with mathematical modeling to effectively design and optimize a photovoltaic-based hydrogen-electricity supply chain [22]. This innovative approach enables simultaneous targeting of vehicle fuel and electricity demands while also identifying suitable locations for supply chain infrastructures. Furthermore, optimization of HSCs with a MILP model can also be integrated with external tools that allow for a more accurate analysis of some of the SC stages. As an example, the authors of [23] calculated the production and distribution costs using two publicly available software, HDSAM and H2A, that can be downloaded from the DOE website [24]. Besides focusing on light- and heavy-duty vehicles, airports can also be viewed as energy hubs where hydrogen can be produced and consumed for different end-use applications. The modeling of a supply chain that serves specifically the airport ecosystem is presented in Ref. [25]. In a similar direction [26], pointed out that, to develop a low-carbon hydrogen supply chain, the waste management process in industrial clusters is significant and cannot be overstated. Multi-objective optimization is applied when more than one aspect needs to be included in the analysis. De-Lèon Almaraz et al. [27] compared two different optimization strategies, i.e., based on lexicographic and ε-constraint methods, to minimize three different objectives: total daily costs, global warming potential, and safety risk. The supply chain's risks are taken into consideration in Ref. [28], where the authors propose a multi-objective MILP model where demand uncertainty is handled with a fuzzy logic procedure. To cope with the high computational effort required by supply chain design optimization problems, Moreno-Benito et al. [29] proposed a multi-period and hierarchical MILP approach. Multi-objective formulation can also be tackled by tailored genetic algorithms as in Ref. [30]. Similarly, a multi-objective optimization problem is addressed using a bi-level formulation and metaheuristics in Ref. [31]. This work also adds some novelties in the modeling of a HSC such as continuous capacities learning rates and emergent technologies. As an alternative to the transportation of pure hydrogen, Hurskainen et al. [32] proposed a techno-economic analysis of the delivery of LOHCs

to a single industrial customer. Results show that LOHCs can significantly reduce long-distance delivery costs. In the modeling of supply chain systems, temporal resolution plays a crucial role as it captures the dynamics of important processes such as the fluctuating nature of renewable energy production and hydrogen storage. In the study conducted by Ricks et al. [33], a capacity expansion and economic dispatch model was applied to assess the environmental impacts of hydrogen production through grid-connected electrolysis. Their results show the importance of incorporating varying levels of spatial, temporal, and operational complexity in the model to minimize the system-level emissions impact of grid-based hydrogen production. Only one study has been found in the literature regarding the implementation of a hydrogen supply chain in the context of Sicily [34]. Two major novelties are added to the traditional MILP model, which is the option of multi-modality for the transportation stage and the use of a node modeling approach. Environmental impact is also assessed through the contribution to climate change made by the hydrogen network operation in Ref. [35] with a life cycle assessment approach. Choosing the broader perspective of network design, Li et al. [36] reviewed the mostly implemented decision variables and objective function formulation in the field of HSC optimization models.

The aforementioned literature focuses on the optimization of light or heavy-duty transport vehicles. However, as highlighted by Herwatz et al. [37], integrating different mobility demands is strategic for achieving economies of scale in hydrogen production and storage appliances serving the transport sector. Aligning with the above-cited literature, this paper proposes an optimization model aimed at minimizing the overall cost of an HSC, but differently from the discussed contributions, it includes passenger trains and urban buses in the analysis. Indeed, fuel demands for trains are nearly deterministic and predictable throughout the year. Aggregating hydrogen demands from regional passenger trains and urban buses presents a novel approach in this field, where the majority of papers solely focus on fuel cell-electric vehicles (FCEVs), i.e., the passenger car market segment. Designing an HSC capable of concurrently serving FCMUs and FCEBs is legitimate, as both applications feature onboard hydrogen storage at 350 bar, thus requiring infrastructures and auxiliary technologies with similar operational performances. Another advantage of coupling the demands for FCMUs and FCEBs within the same HSC is the ease of computing their daily demands, given these values remain fairly consistent over the year. The decision to include the railway sector in the HSC design is driven by the Italian normative scenario, which advocates for the adoption of hydrogen trains, especially in Southern Italy, where a radical transformation of the mobility sector is crucial for fostering the economic growth of the area. In accordance with this discussion, the model presented in this study aims to design the HSC in terms of the optimal number, size, and location of hydrogen production facilities, as well as the optimal hydrogen distribution and refueling infrastructures in Sicily. In more detail, this work delves into the following issues, open to debate:

1. Most discussions in the HSC literature contemplate the production of hydrogen from a broad spectrum of technical processes, encompassing both renewable (wind-/solar-powered electrolysis plants, biomass gasification) and non-renewable (coal gasification, steam methane reforming) sources. Hydrogen could significantly contribute to the sustainable energy transition, especially when produced using renewable primary energy sources. In this study, only wind energy is utilized to produce green hydrogen via a water electrolyzer at each hydrogen production site. This choice is particularly pertinent for the Sicilian case study, given the high availability of wind farms that have been decommissioned due to grid congestion issues in the past.
2. Thus, the model presented in this paper is constructed to fully adopt existing wind farms. Contrary to the cited literature, usually envisioning the installation of new wind turbines or, generally, the construction of new renewable plants, the HSC design model developed here aims to valorize the existing facilities and auxiliary infrastructures. This approach significantly reduces investment costs while maximizing the utilization of already available resources in the selected region and accurately localizing each hydrogen production site on the map. Finally, the outcomes of such a model can indicate the total capacity that needs to be established in each region to meet the hydrogen demand of the chosen final uses. The capacity expansion of electricity production facilities is not considered since only existing wind farms and power grids are modeled.
3. Another distinguishing factor lies in the geographical approach used; here, indeed, the model is shaped around existing geographical constraints, yielding more reliable results, and directing towards effective utilization for train and bus companies.

2. Materials and Methods

The design of the HSC is explored to assess the viability of establishing hydrogen infrastructures to cater to the rail and bus sectors, leveraging the potential production capabilities of pre-existing wind farms in Sicily. Fig. 1 provides a synopsis of the modelling framework employed in this study.

The process delineated for the HSC design comprises three principal stages: the input data stage, problem formulation and optimization, and results manipulation. The input block pertains to the data and chosen structure required to build the model. Initially, a thorough geographic breakdown of the region where the HSC is to be designed is imperative. This encompasses a territorial map pertinent to the analysis, reflecting specific regional expanses (here aligned with the administrative boundaries of Sicilian cities) along with details on train railways and bus routes. Given the spatial information, hydrogen demands for FCEBs and FCMUs need to be ascertained for each region and utilized as input for the optimization. Subsequently, renewable sites designated for hydrogen production must be identified, particularly requiring hourly production profiles and plant locations as feed-in data for the proposed model. Additionally, techno-economic and environmental data are essential for advancing the optimization, encompassing power size, costs, and emission rates.

The HSC optimization problem for the trains and buses is formulated as a spatially explicit MILP model, employing the GAMS Studio 37.1.0 language [38] with CPLEX 20.1.0.1 [39] as the solver. Various demand scenarios, as delineated in the second block of Fig. 1, can be optimized. The optimization problem minimizes the total cost of the entire HSC per day, concurrently accounting for the tons of CO_2 avoided through the utilization of electricity produced with renewable sources. Additionally, the location, size, and the number of production and refueling facilities are determined, alongside the resulting hydrogen flows regarding eligible routes and transport modes (liquified/gaseous hydrogen). Data are visualized in MATLAB and Excel, yielding hydrogen flow maps for the prompt localization of routes, and number, type, and size of electrolyzers.

Delving deeper, Fig. 2 delineates the stages under consideration in this study for the HSC design. As illustrated, the HSC optimally leverages existing Sicilian wind farms for the electrical supply to alkaline electrolyzers, augmented by connection with the main grid to counterbalance the fluctuating nature and unavailability of wind production.

It's noteworthy that the wind farms examined in this analysis remain non-operational for a substantial part of the year. Hence, a fundamental assumption within the model is that the energy produced on the selected average day would be curtailed if not utilized immediately. Consequently, in the average day scenario, all the renewable electricity produced could be employed to produce low-carbon hydrogen via water electrolysis, physically connected to the wind plant. All electrolyzers also maintain connection to the power grid, which compensates for the intermittent nature of renewable production by consistently providing the electrolyzer's nominal power throughout the day. The maximum hydrogen quantity producible by each wind farm operating at full

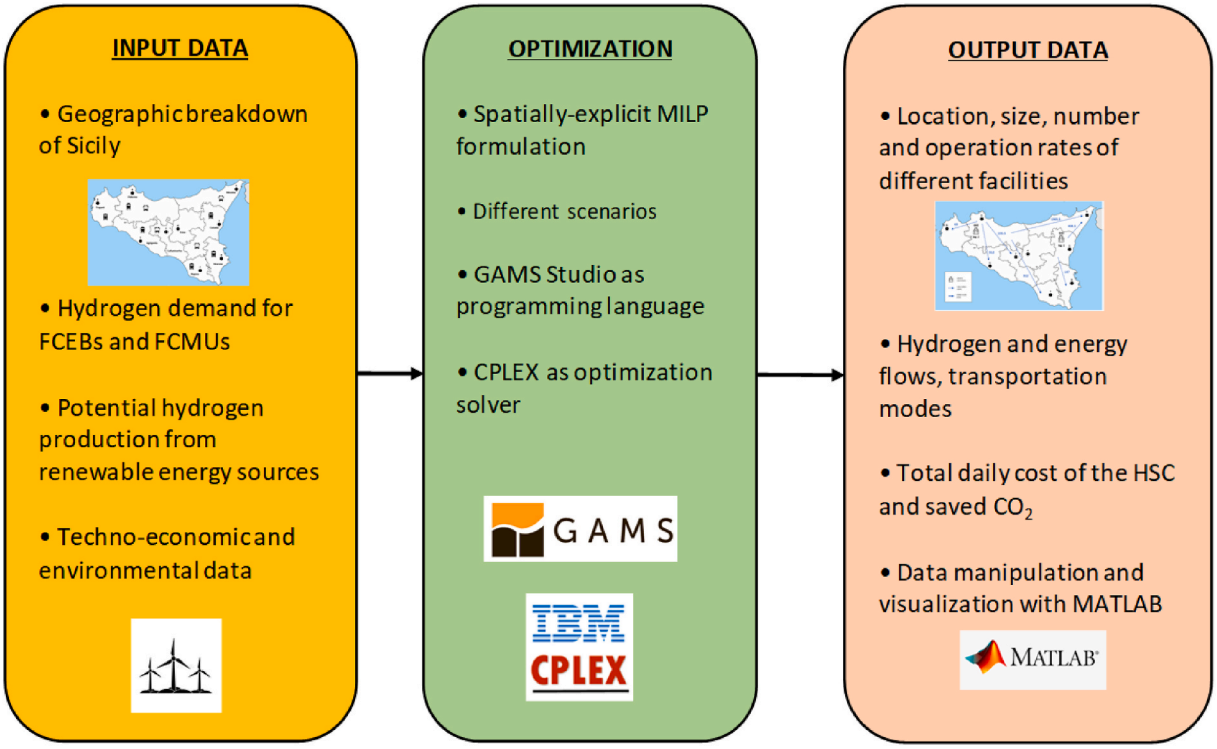

Fig. 1. An overview of the adopted modeling framework.

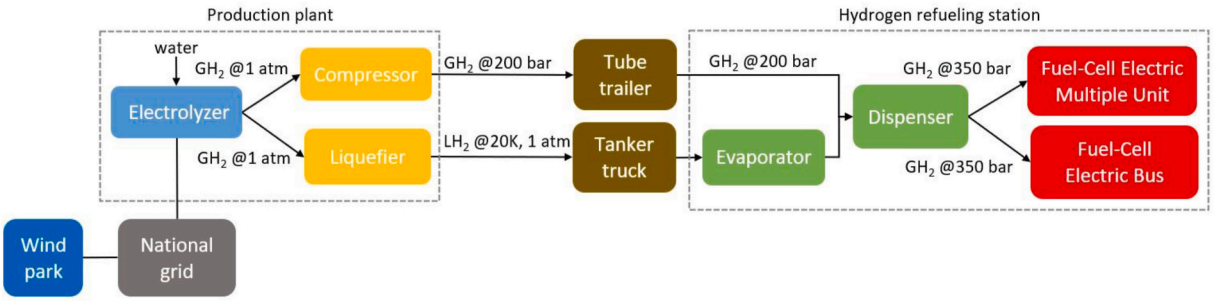

Fig. 2. HSC superstructure implemented in the optimization model.

capacity during the selected average day is computed by dividing the electricity production of the wind farm by the efficiency of the electrolyzer technology in kWh/kgH_2.

Pertaining to the technological selection underpinning the HSC structure, alkaline technologies are favored over PEME (Polymer Electrolyte Membrane Electrolyzers) and SOEC (Solid Oxide Electrolyzers Cell) for four reasons: (i) in their current form, they represent a mature, reliable, and safe technology [40,41] with production capacities extending to the megawatt scale [40], (ii) the absence of CRM (Critical Raw Materials), noble/precious metals (platinum, iridium) for the electrode catalysts, thereby reducing overall manufacturing costs; specifically, around 1000 – 1400 €/kW compared to 1750 €/ kW for PEME [41,42], (iii) they exhibit a higher lifespan of 10 – 15 years compared to PEME technologies [40,43], and (iv) the hydrogen produced has a purity exceeding 99.94% [44], rendering it suitable for utilization in a hydrogen fuel cell.

Gaseous hydrogen (GH_2) is produced at atmospheric pressure by electrolyzers powered by electricity from wind farms. Given the fluctuating nature of wind, hydrogen production can be supplemented with electricity from the main grid, making the grid connection essential to ensure constant nominal power to the electrolyzers. It is assumed that hydrogen conditioning facilities, i.e., the compressor and the liquefier, are situated near the electrolyzers. Depending on the mode of transportation, i.e., for gaseous or liquid hydrogen, the plant should have either a compressor or a liquefier. The compressor increases the hydrogen pressure to 200 bar, after which it is transported by tube trailers with a net capacity of 1000 kg H_2 [12,45]. Liquefaction of H_2, for transporting liquid hydrogen (LH_2) is technologically more complex than gaseous compression, and to be effective, should operate until the temperature of 20 K, with a net capacity of 4000 kg H_2 for transportation, typically carried out by tanker trucks [12,46]. In this study, the transportation of pure hydrogen via a dedicated pipeline network is not contemplated in the establishment of a new hydrogen supply chain due to high complexity and investment costs entailed in constructing such a pipeline network. This assumption aligns with the phased approach embraced by most extant hydrogen supply chains [47]. Per this concept, the initial phase of a supply chain, typified by relatively low hydrogen demand, can be effectively catered to using highly flexible transportation modes such as trucks. As hydrogen volume increases, more expensive and expansive infrastructure will be progressively developed to cater the growing demand. As a further remark, this research distinctly concentrates on the hydrogen demand from the local

and regional passenger transportation sector. Hence, the final stage of the HSC encompasses the refueling operations, generally in proximity to rail or bus depots. Post transportation, compressed H_2 from tube trailers requires further compression to 350 bar to align with the FCMUs or FCEBs tanks [48,49]. Similarly, the requisite operating conditions for the tanks transporting LH_2 are attained by installing an evaporator at the refueling station. The HSC design problem is formulated as a MILP model, trailing the approach of Almansoori and Shah [15] and Moreno-Benito et al. [29]. To design the HSC, input data concerning hydrogen demands and the geographic territory are crucial. The demand from FCEBs is considered an on-top hydrogen demand to increase HSC economies of scale, as suggested in Ref. [37]. It is notable that hydrogen demands of FCMUs and FCEBs can be deemed deterministic as the daily covered distances per vehicle and numbers of daily trains or buses remain largely constant throughout the year. As delineated, Sicily is the focus of this study, and for this purpose, it has been segmented into specific subregions, to which a daily hydrogen demand has been assigned and calculated as:

$$D_{H_2} = FE \cdot dist \cdot HU \tag{1}$$

The daily hydrogen demand D_{H_2} is calculated by multiplying the fuel economy FE, which expresses the amount of kilogram of hydrogen consumed by each vehicle to cover a distance of 1 km. The other multiplying factors in the equation are the daily average covered distance, dist, and the number of buses and trains, HU.

The objective function is formulated to minimize the total daily costs of the HSC, as follows:

$$\min(\text{HSC daily costs}) = \frac{FCC + TCC}{\alpha \cdot ccf} + POC + TOC \tag{2}$$

The sum of facilities capital costs FCC and transport capital costs TCC is divided by α, which represents the operating period of the network in days per year, and the capital charge factor pertaining to the supply chain investment, ccf. This parameter is crucial for annualizing the total investment cost of the supply chain. The capital cost variables (FCC, TCC) and the operating cost variables (POC, TOC) are respectively impacted by the activation/deactivation of infrastructures at each stage of the supply chain and by the daily production and flow rates of hydrogen for each node and link of the network. It is important to acknowledge that the capital and operating costs associated with the end-users, such as trains and buses, have not been incorporated within the optimization process. This exclusion is due to these costs being treated as fixed parameters that lack influence over the optimization outcome.

The cost components of the objective function in Eq. (2) are detailed below. Starting from the facilities' capital costs FCC, they can be calculated as:

$$FCC = \sum_g \sum_i \sum_j pcc_{ij} \cdot NP_{gij} + \sum_g \sum_i rcc_i \cdot NRS_{gi} \tag{3}$$

In which the cost of establishing hydrogen production facilities pcc_{ij} and hydrogen refueling stations rcc_i are multiplied by the actual number of installed facilities or refueling stations in each location, respectively NP_{gij} and NRS_{gi}, specified in terms of the hydrogen physical form i, size j of the production facilities, and location g.

The transport capital costs TCC are calculated as in Eq. (5):

$$TCC = \sum_g \sum_{g'} \sum_i NTU_{gg'i} \cdot \sum_i tucc_i \tag{4}$$

In particular, these are obtained by multiplying the number of transportation units $NTU_{gg'i}$ by the related investment cost $tucc_i$, for each physical form i of hydrogen, and each established transportation link from location g to location g'.

The number of transportation units for each established route, $NTU_{gg'i}$, is reported as in Eq. (6):

$$NTU_{gg'i} \geq \frac{HF_{gg'i}}{tucap_i^{max}}, \ \forall g, g', i \tag{5}$$

They are derived from the ratio between the daily hydrogen flows, $HF_{gg'i}$, occurring between the locations g and g', and the maximum delivery capacity of the transport unit, $tucap_i^{max}$, both at varying the physical form i in which hydrogen is delivered.

The operation costs for production POC are obtained by multiplying the daily production rate of hydrogen HPR_{gij} and the unit production cost upc_{ij}, both specified for the physical form i of hydrogen, the size j of the production facilities, and the location g.

$$POC = \sum_g \sum_i \sum_j upc_{ij} \cdot HPR_{gij} \tag{6}$$

The transport operating costs TOC are calculated as the sum of the transport fuel cost TFC, the transport labor cost TLC, i.e., the cost of the driver, and the cost for maintenance TMC, as in Eq. (7):

$$TOC = TFC + TLC + TMC \tag{7}$$

The cost items in Eq. (7) depend on the traveled distance per day.

More in detail, they are calculated as follows. The transport fuel cost TFC is:

$$TFC = \sum_g \sum_{g'} \sum_i fuel_i \cdot \left(\frac{2 \cdot dist_{gg'} \cdot HF_{gg'i}}{fc_i \cdot tucap_i^{max}} \right) \tag{8}$$

As can be observed from Eq. (8), the transport fuel cost, TFC, depends on the unit price of the fuel $fuel_i$, fuel consumption per km fc_i, the daily hydrogen flows $HF_{gg'i}$, and the transport unit's maximum capacity $tucap_i^{max}$, all specified for each hydrogen physical form i, and on the distances covered by the transportation unit $dist_{gg'}$ from location g to location g'.

The transport labor cost TLC is given as:

$$TLC = \sum_g \sum_{g'} \sum_i driver_i \cdot \frac{HF_{gg'i}}{tucap_i^{max}} \cdot \left(\frac{2 \cdot dist_{gg'}}{speed_i} + lutime_i \right) \tag{9}$$

Eq. (9) considers the hourly cost of the driver, $driver_i$, the average speed $speed_i$, the distances between the two locations g and g' locations, $dist_{gg'}$, the loading or unloading time of a transport unit delivering hydrogen in the physical form i, $lutime_i$, the hydrogen flow from location g to g' considering the physical form i, $HF_{gg'i}$, and transport unit maximum delivery capacity $tucap_i^{max}$, associated with the specific hydrogen form i.

Finally, the daily maintenance costs, TMC, are calculated as follows:

$$TMC = \sum_g \sum_{g'} \sum_i mc_i \cdot \left(\frac{2 \cdot dist_{gg'} \cdot HF_{gg'i}}{tucap_i^{max}} \right) \tag{10}$$

The expression for Eq. (10) is similar to Eq, (8), except for the value of the maintenance operation per km, mc_i.

After the definition of the objective function, the following balance equations and constraints of the model are presented. Eq. (11) reports the mass balance equation for hydrogen production. In particular:

$$\sum_j HPR_{gij} + \sum_{g'} HF_{g'gi} = HDEM_{gi} + \sum_{g'} HF_{gg'i}, \ \forall g, i \tag{11}$$

The sum of hydrogen in the physical form i produced at location g in a facility of size j, HPR_{gij}, and of hydrogen flow in the physical form i arriving at location g from every other possible location g', $HF_{g'gi}$, must be equal to the sum of the demand of hydrogen in the same physical form i and produced at the same location g, $HDEM_{gi}$, and the hydrogen flow from location g to every other location g', in the physical form i, $HF_{gg'i}$.

$$\sum_i HDEM_{gi} = hdem_g, \ \forall g \tag{12}$$

The total demand for hydrogen in the physical form i, $hdem_{gi}$, must balance the hydrogen demand of different physical forms i, $HDEM_{gi}$, in each location g, as expressed in Eq. (12). More in detail, Eq. (12) is needed to disaggregate the total demand $hdem_g$ and so to distinguish whether a refueling station is receiving hydrogen in liquid or gaseous form. The formulation of this constraint does not affect the optimized results since it is solely needed to streamline the process of feeding input data to the model. Eq. (18) counts the number and types of hydrogen refueling stations in each location g, NRS_{gi}, based on the maximum capacity of the refueling station per hydrogen physical form i, $rcap_i^{max}$, and on the disaggregated demand $HDEM_{gi}$. It can be observed from Eq. (13) that the hydrogen refueling station can either receive liquid or gaseous hydrogen: two different modes that impact differently on capital costs of the objective function

$$HDEM_{gi} \leq NRS_{gi} \cdot rcap_i^{max}, \ \forall i, g \tag{13}$$

Eq. (14) expresses the constraint for which, when hydrogen is produced by small facilities, i.e., i = 1, it can only be used to satisfy local demand.

$$HPR_{gij} \leq HDEM_{gi}, \ \forall i, g \text{ and } j = 1 \tag{14}$$

The hydrogen production rate HPR_{gij}, in the physical form i, produced in the facility j at location g has a lower and upper limit, expressed as:

$$pcap_{ij}^{min} \cdot NP_{gij} \leq HPR_{gij} \leq pcap_{ij}^{max} \cdot NP_{gij}, \ \forall i, j, g \tag{15}$$

In particular, it is limited by the number of existing production facilities, NP_{gij}, constrained by lower and upper production capacities, respectively $pcap_{ij}^{min}$ and $pcap_{ij}^{max}$.

The hydrogen production rate HPR_{gij} is also characterized by the following constraint:

$$\sum_{ij} HPR_{gij} \leq res_g^{max}, \ \forall g \tag{16}$$

Eq. (16) adds to Eq. (14) that the hydrogen production rate, HPR_{gij}, cannot be higher than the maximum daily production capacity of hydrogen produced from the renewable energy sources available in each location, res_g^{max}.

Eq. (17) is needed to link the binary variable $Y_{gg'i}$, referring to the established connection between two locations, to the continuous variable $HF_{gg'i}$, referring to the hydrogen flow between the same locations:

$$Y_{gg'i} \leq HF_{gg'i} \leq flow_i^{max} \cdot Y_{gg'i}, \ \forall g, g', i \tag{17}$$

If a transportation route is not established between two locations, the binary variable would be equal to zero. The maximum flow rate, $flow_i^{max}$, is fixed for each transportation mode, as done in Ref. [15]. Then, it is worth noting that the model proposed in this study does not consider a minimum hydrogen flow rate among locations.

Eq. (18) poses the constraint for which hydrogen flows between two locations, $Y_{gg'i}$, can only occur in one direction and not, simultaneously, in the opposite.

$$Y_{gg'i} + Y_{g'gi} \leq 1, \ \forall i, g, g' \tag{18}$$

Finally, all continuous and integer variables are constrained to be non-negative.

3. Case study

The optimization model delineating in the preceding section has been implemented for Sicily, the southernmost region of Italy, encompassing an area of 25,711 km^2. Sicily holds enormous potential for production zero- or low-carbon hydrogen through electrolysis powered by renewable energy sources [50]. It is particularly distinguished as one of the windiest regions in Italy [51]. The substantial electricity production from wind is further corroborated by the fact that a notable number of Sicilian wind farms that have been decommissioned due to an unbalance with the main grid, which cannot accommodate additional electricity inputs [52]. This aspect highlights both the high wind capacity in Sicily, resulting in higher full load hours compared to other renewable sources, and the significant potential for green hydrogen production from wind resources within the region. The costs associated with technologies, auxiliary services, and infrastructure supporting hydrogen production and transportation are pivotal. In this scenario, the sustainable utilization of existing wind farms and supporting infrastructures emerges as essential in propelling the transition toward hydrogen-based mobility, especially in the short term.

Delving deeper into the detail of the HSC modeling, a substantial effort is necessitated to collect input data, such as technical specifications from datasheets or the existing literature, alongside reliable boundary conditions, parameters, and constraints formulated in adherence to technical reports and governmental bodies. Commencing with the territorial constraints, the examined island has been partitioned into distinct zones, each corresponding to the administrative boundaries of a region. The geographical breakdown of Sicily is illustrated in Fig. 3, showcasing the borders of the 9 subregions, with the local administration of each Sicilian city denoted by a black dot. This approach obviates the need for the conventional regular and quadrangular grids commonly used in the literature for modeling purposes, thereby accommodating the specific requisites or constraints and variables unique to the subregions. Furthermore, employing this spatial discretization facilitates the precise identification of linking routes, as well as the central stations that can be strategic for refueling in terms of location and proximity to wind farms. While this methodology is not prevalent in the literature centered on HSC, there are instances, such as the work of De-Leon Almaraz [27], that echo a similar approach.

The total installed wind farm capacity in Sicily has been calculated from a data collection campaign of the GSE [52], as reported in Table 1.

As mentioned earlier, the entire electric energy generated by each wind farm is utilized to produce hydrogen via an electrolyzer. To determine the electric energy that can be transmitted from a wind farm to an electrolyzer, a simulation is conducted, factoring in the electrolyzer operating at its nominal power throughout the chosen average day. The maximum daily production is subsequently deduced by dividing the energy value derived from the simulation by the specific electrical consumption of an alkaline electrolyzer (as shown in Table 5). Under typical Sicilian weather conditions, the average daily hydrogen production per installed MW of wind capacity is pegged at 78 kg, serving as a cornerstone to compute the potential maximum hydrogen production capacity across all wind farms.

In addition to pinpointing the location of wind farms, it is imperative to delineate the relative distance between subregions in Sicily to endeavor the minimization of operational costs for tube-trailer and tanker trucks. The outcomes are tabulated in Table 2.

Within each subregion, the hydrogen demand for FCMUs and FCEBs has been computed in accordance with Eq. (1) and is reported in Table 3. It is notable that the subregions 2, 4, and 5, corresponding to Caltanissetta, Enna, and Messina respectively, lack a hydrogen demand for FCMUs, as these areas do not possess non-electrified routes slated for conversion. As delineated in Table 3, three distinct scenarios have been considered for the optimization. In the initial case, Scenario 1, non-electrified railway routes alongside FCMU trains are taken into account for the demand estimation of the HSC. For this scenario, the equivalent hydrogen demand for all railway routes is depicted in Table 4. The subsequent case, Scenario 2, considers the demand derived from the bus routes, FCEBs. The hydrogen demand for FCEBs (and FCMUs) is determined as per Eq. (1), where the daily average distance covered per bus is pegged at 250 km/day [53], and the number of buses in each sub-region is sourced from official public transport websites. Scenario 3 couples together the demand for FCMUs and FCEBs.

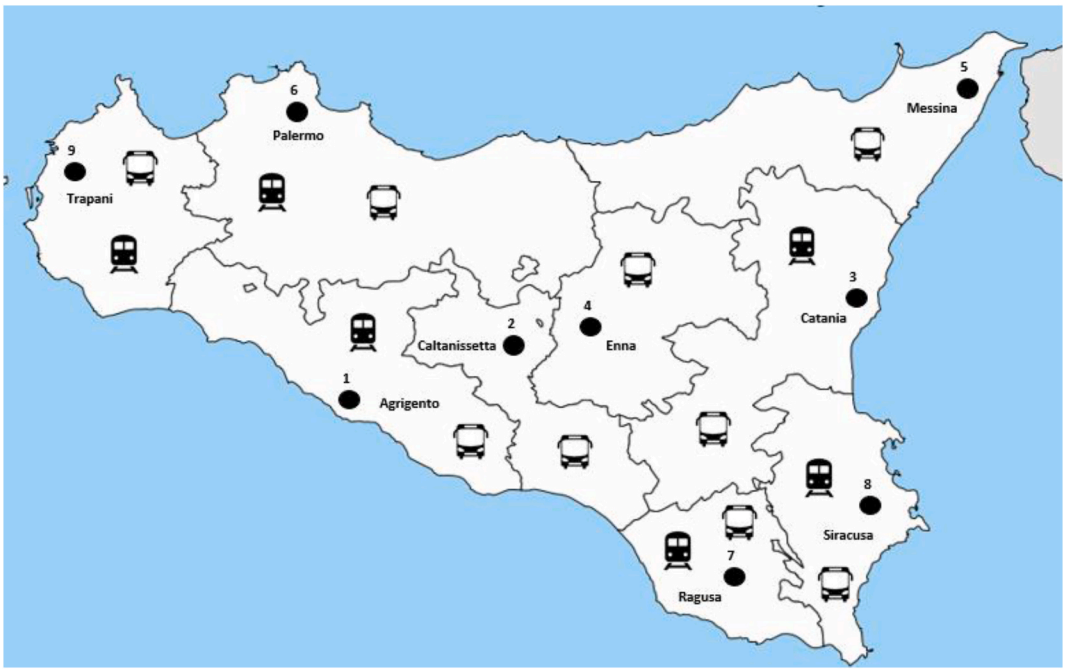

Fig. 3. Geographic breakdown of the identified subregions in Sicily with end-use type of demand.

Table 1
Total installed wind farm capacity in Sicilian provinces and daily hydrogen production.

ID	Installed capacity [MW]	Daily hydrogen production capacity [kgH_2 /day]
1	319.8	25010.51
2	56.77	4439.80
3	247.6	19363.99
4	126.5	9893.15
5	213.45	16693.23
6	352.401	27560.13
7	2.04	159.54
8	142.16	11117.87
9	313.62	24527.19

More detailed information on the data can be found in Table 4, where the non-electrified routes in Sicily have been identified in terms of length, number of trains serving these routes per day, and the derived hydrogen demand.

Beyond the delineation of boundary conditions for HSC design, the computation of hydrogen demand, and the definition of scenarios, it is crucial to elaborate on the selection of the electrolyzers. In this study, three sizes of electrolyzers have been considered: small, medium, and large, with power capacities of 1 MW, 5 MW, and 20 MW respectively, across each scenario. It is pertinent to recall that small electrolyzers can only be installed directly at the point of demand (i.e., refueling station) to cater to the local hydrogen demand. Analogous to other studies in the pertinent literature, the preceding assumption has been defined arbitrarily, given the size and capacity of such an electrolyzer render it particularly apt for installation directly at the point of demand, which, in this instance, refers to a refueling station. This is modeled via Eq. (14). Further details on the techno-economic data concerning the hydrogen production facilities selected for this study are presented in Table 5, below.

The shaft power, i.e., the power requirement and the costs for compressor unit design is calculated as in Ref. [57], considering the inlet and outlet pressure of hydrogen, respectively 1 bar and 200 bar. The specific energy consumption for the compression and liquefaction unit is fixed and equal to 1.9 kWh/kgH_2 [24] and 11 kWh/kgH_2 [58], respectively. The specific capital cost of a liquefier has been assumed 5000 €/(kgH_2/day) [58].

More details on the cost values assumed in this study and used to optimize the HSC, specifically concerning the production stage, are reported in the following Tables, at varying electrolyzer sizes and for liquified and gaseous hydrogen. In detail, Table 6 reports the investment costs of production facilities, and Table 7 the hydrogen production costs per kg of produced H_2.

Tables 8 and 9 report the minimum and maximum production capacities, respectively. Once more, values are presented for the three selected electrolyzer sizes, specified for both liquified and gaseous hydrogen. The values in Table 9 are computed utilizing hydrogen hourly production per MW of installed electrolyzer, as illustrated in Table 5.

Table 2
Euclidean distance between subregions in [km].

ID	1	2	3	4	5	6	7	8	9
1	–	47.47	135.31	68.48	199.79	90.99	110.58	154.53	121.82
2	47.47	–	90.39	21.01	152.58	93.15	85.97	118.50	148.17
3	135.31	90.39	–	71.50	87.15	166.82	72.24	51.91	233.25
4	68.48	21.01	71.50	–	131.76	101.57	81.64	105.36	163.01
5	199.79	152.58	87.15	131.76	–	192.79	159.38	127.72	266.62
6	90.99	93.15	166.82	101.57	192.79	–	179.11	206.72	73.99
7	110.58	85.97	72.24	81.64	159.38	179.11	–	53.01	229.66
8	154.53	118.50	51.91	105.36	127.72	206.72	53.01	–	266.66
9	121.82	148.17	233.25	163.01	266.62	73.99	229.66	266.66	–

Table 3
Hydrogen daily demand for each scenario.

ID	Subregion	Scenario 1 (FCMUs) [kgH_2 /day]	Scenario 2 (FCEBs) [kgH_2 /day]	Scenario 3 (FCMUs and FCEBs) [kgH_2 /day]
1	Agrigento	312	2403	2715
2	Caltanissetta	0	160.2	160.2
3	Catania	1498.5	7903.2	9401.7
4	Enna	0	152	152
5	Messina	0	2776.8	2776.8
6	Palermo	333	16927.8	17260.8
7	Ragusa	312	2363	2675
8	Siracusa	147	2303	2450
9	Trapani	63	1903	1966

Table 4
Non-electrified railway lines in Sicily and daily hydrogen demand for FCMUs [54,55].

Name	Length [km]	Number of trains per day	Hydrogen demand [kgH_2 /day]
Ferrovia Circumetnea	110	45	1498.5
Trapani-Alcamo	35	6	63
Trapani-Palermo	74	15	333
Siracusa-Gela-Canicattì	130	8	312
Lentini-Caltagirone-Gela	70	7	147

Table 5
Techno-economic parameters of hydrogen production facilities [56].

Parameter	UoM	Alkaline electrolyzer size		
		1 MW	5 MW	20 MW
Specific energy consumption	[kWh /kgH_2]	58	52	51
Hydrogen hourly production	[(kgH_2 /hr) /MW]	18		
Water consumption	[l /kgH_2]	15		
Electrolyser normalized CAPEX	[€ /kW]	1200	830	750
Electrolyser total CAPEX	[€]	1,200,000	4,150,000	15,000,000
Compressor CAPEX	[€]	166,780.45	833,902.23	3,335,608.92
Liquefier CAPEX	[€]	2,160,000	10,800,000	43,200,000

Table 6
Hydrogen production capital costs [€].

Physical form	Size		
	Small	Medium	Big
LH_2	3,360,000.00	14,950,000.00	58,200,000.00
GH_2	1,200,065.53	4,150,327.66	15,001,310.65

Table 7
Hydrogen production operational costs [€ /kgH_2].

Physical form	Size		
	Small	Medium	Big
LH_2	3.43	3.14	3.09
GH_2	2.90	2.61	2.56

Table 8
Minimum production capacity $pcap_{ij}^{min}$ [kgH_2 /day].

Physical form	Size		
	Small	Medium	Big
LH_2	100	500	1000
GH_2	100	500	1000

Table 9
Maximum production capacity $pcap_{ij}^{max}$ [kgH_2 /day].

Physical form	Size		
	Small	Medium	Big
LH_2	432	2160	8640
GH_2	432	2160	8640

After being produced, hydrogen needs to be transported according to its physical form, i.e., liquified or gaseous hydrogen. The main techno-economic parameters adopted to feed the optimization model have been elaborated from the existing literature and manuals. Values and sources are reported in Table 10, below. Regarding the refueling station, the main input data has been collected and reported in Table 11.

Finally, other parameters, such as water and wind electricity prices, as well as the price of electricity from the main grid and the related emission factor are reported in Table 12, with sources reported in the last column.

4. Results and discussion

The optimization model developed in this study aims to outline a possible configuration of a HSC for railway and bus routes in Sicily, leveraging the substantial potential of electricity from pre-existing wind farms. Hydrogen is envisioned to be supplied to FCMUs and FCEBs via tanker trucks and tube trailers, in liquified or compressed form respectively. The total cost of the HSC, encompassing both capital and operating costs, is minimized across the production, transportation, and refueling stages. Hereafter, the optimized HSC configurations for the three identified scenarios in Table 3 are presented and discussed. The results from the optimization are depicted on geographical maps to accentuate the physical forms of hydrogen, routes, electrolyzer size, and number. The maps have been crafted using a consistent legend to facilitate cross-comparison and discussion. Specifically, electrolyzers are represented as squares, pentagons, and hexagons, corresponding to small, medium, and large sizes, respectively. The optimal number of electrolyzers to be installed at a selected location (primarily dependent on the existing wind farm) is encapsulated within each of these mentioned shapes. Dotted or continuous red lines signify the gaseous or

Table 10
Techno-economic parameters of transportation modes [29,43,59,60].

Parameter	UoM	Tanker truck LH_2	Tube trailer GH_2
Transport unit capacity $tucap_i^{max}$	[kgH_2]	4300	1000
Average speed $speed_i$	[km /hr]	50	50
Loading/Unloading time $lutime_i$	[hr]	3	1.5
Driver cost $driver_i$	[€ /hr]	21	21
Maintenance expenses mc_i	[€ /km]	0.08	0.08
Fuel consumption fc_i	[km /l]	2.3	2.3
Maximum flow rate $flow_i^{max}$	[kgH_2/day]	960,000.00	960,000.00
Transport unit capital costs $tucc_i$	[€]	908,951	563,550
Fuel price $fuel_i$	[€ /l]	1.725	1.725
Transport emission factor tef_i	[$kgCO_2$ /km]	1.12	1.12

Table 11
Techno-economic parameters of hydrogen refueling station [61].

Parameter	UoM	Value	
		LH_2	GH_2
Capital costs rcc_i	[€]	1,900,000	1,400,000
Maximum daily capacity $rcap_i^{max}$	[kgH_2 /day]	1400	770

Table 12
Other parameters used in the model.

Parameter	UoM	Value
Fuel economy for FCEBs FE	[kgH_2 /km]	0.089 [62]
Fuel economy for FCMUs FE	[kgH_2 /km]	0.3 [63]
Operating period α	[day/year]	365
Capital charge factor ccf	[year]	3 [15]
Water price	[€ /l]	0.00129 [64]
Wind electricity price	[€ /kWh_e]	0.05 [52]
Grid electricity price	[€ /kWh_e]	0.187 [65]
Saved emissions from wind	[$kgCO_{2eq}$ /MWh_e]	536 [51]

liquified transportation mode, via tube trailers or tanker trucks, respectively, with the number above each arrow indicating the daily hydrogen flow rate, expressed in kgH_2/day. It is essential to underline that in the illustrated maps, the installation of any electrolyzer entails the concurrent setup of all auxiliary services and components, such as compressors or liquefiers constituting the hydrogen production plant. Thus, each node marked with an electrolyzer symbol on the optimized maps signifies a fully operational hydrogen production facility, equipped with all the requisite components to produce either liquid or gaseous hydrogen at 200 bar.

The inference drawn from the results of the supply chain optimization model hinges substantially on two key determinants: the availability of primary energy from the wind farm and the level of hydrogen demand, both of which fluctuate across different nodes in the network.

The optimized HSC design for Scenario 1, i.e., the scenario solely considering the hydrogen demand from FCMUs, is delineated in Fig. 4. As illustrated, the map outlines the administrative boundaries of Sicilian subregion with a black dot marking the administrative center of the main municipality of the subregion.

Upon an initial overview of the map in Fig. 4, it becomes evident that the favored transportation mode entails the gaseous form of hydrogen via tube trailers, a trend that extends to the subsequent two scenarios. Furthermore, it is clear that, except for subregions 1 and 6, the hydrogen supply is predominantly facilitated by the production facility situated in subregion 3, where the deployment of a medium-sized electrolyzer emerges as the most cost-effective solution, thereby centralizing hydrogen production for the entire network.

The strategic decision to install a larger electrolyzer in subregion 3 and distribute hydrogen to the rest of the network, despite the elongated transportation distances (*e.g.*, from node 3 to node 9), materializes as a cost-optimal design outcome. This is attributable to subregion 3, capable of serving as a hydrogen production hub for the entire region, also in light of the low demand level of the analyzed scenario. The bulk of the demand is clustered around subregion 3 (refer to Table 3), rendering it apt to serve as a hydrogen production hub for neighboring sub-regions, such as nodes 7 and 8. Hence, a larger electrolyzer is deployed there to cater the local demand and allocate the surplus production to serve nearby nodes 7 and 8, as well as the more distant node 9, which necessitates a smaller daily hydrogen share (63 kgH_2/day). Conversely, the installation of larger electrolyzers in nodes 1 and 6 would not have been cost-efficient due to the low level of local demand and the suitable distance from the actual demand hub, consisting of subregions 3, 7, and 8.

As an outcome of the optimization, having dedicated electrolyzer where the hydrogen demand is high allows for the local satisfaction of demand, while transportation is leveraged to deliver surplus production to other nodes in the network. The optimization accentuates the cost-effectiveness of installing production facilities since their associated investment costs bear a significant impact on the objective function formulation, Eq. (2).

As a concluding note, subregions 2, 4, and 5 neither exhibit hydrogen deliveries or production plants owing to the lack of non-electrified railways within their perimeters, rendering their demand null in Scenario 1 (see Table 3).

The HSC design is now commented on for Scenario 2, wherein only bus routes are considered. The optimized results for FCEBs are visually delineated in Fig. 5.

In the scenario concerning FCEBs, the transportation of compressed-gaseous hydrogen from the point of production to the point of use is favored over the liquefied form hydrogen to achieve the minimization of

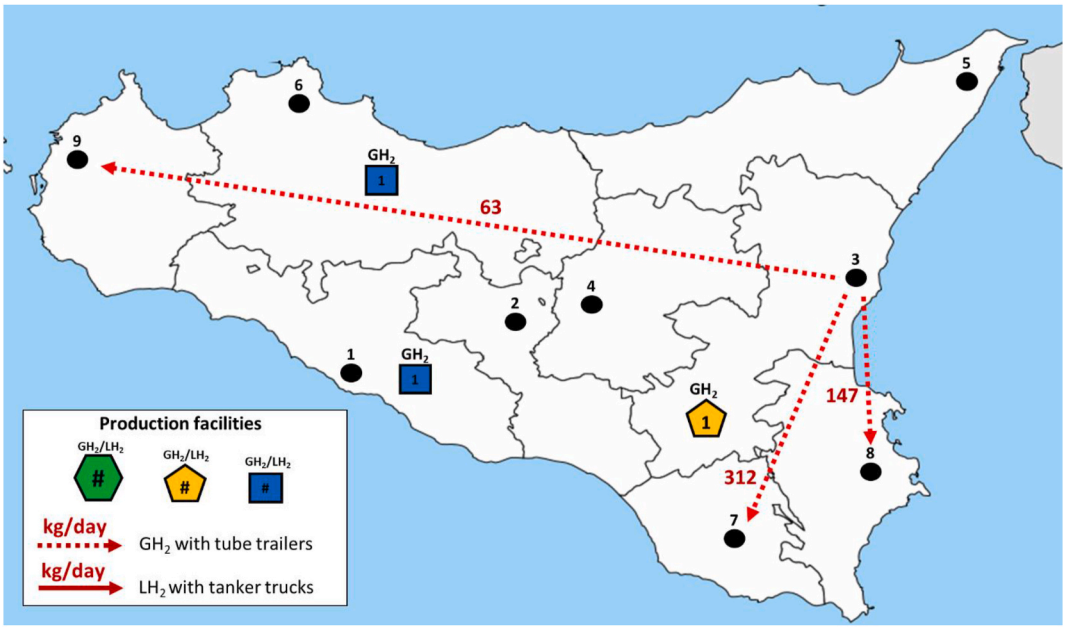

Fig. 4. Optimized HSC for Scenario 1, considering only FCMUs.

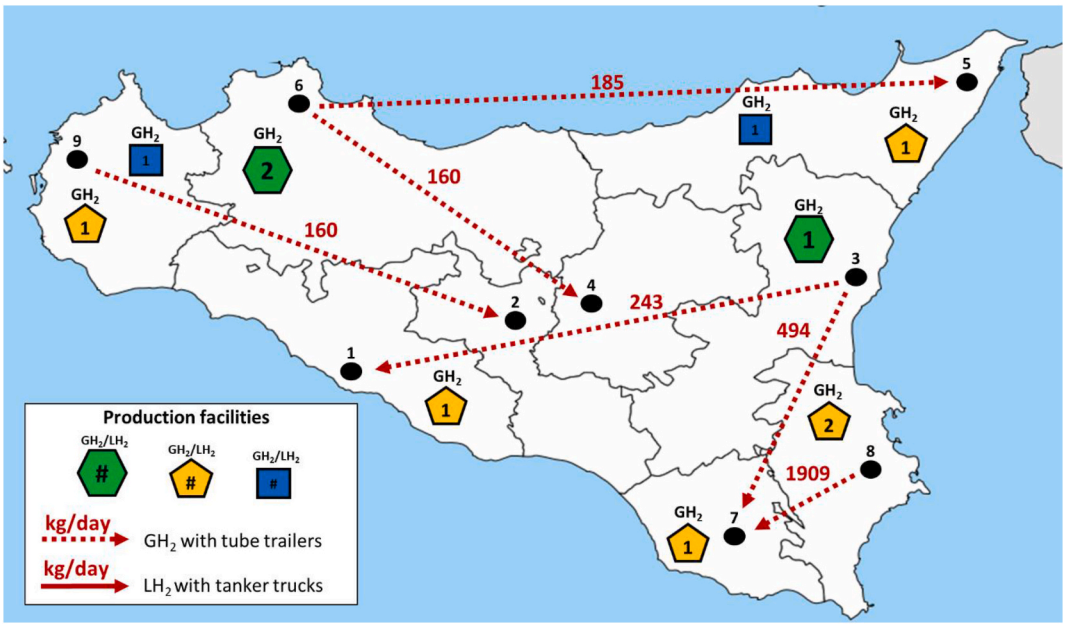

Fig. 5. Optimized HSC for Scenario 2, considering only FCEBs.

the total daily cost of the HSC. Despite tube trailers conveying lesser amounts of hydrogen compared to tanker trucks, which results in higher transport costs per kgH_2 carried, they prove to be more cost-effective from a supply chain standpoint when compared to the costs entailed by the liquefaction stage. Given that liquefaction units are significantly more expensive than compression units, the production of gaseous hydrogen is preferred over liquid hydrogen when the objective function is steered towards minimizing the total daily cost of the HSC. In this scenario, node 6 manifests the highest demand, followed by node 3, which explains why the largest production facilities are installed in these two subregions.

Furthermore, transportation links with distances shorter than those delineated in the optimized network, for instance, from node 3 to 4 rather than from node 6 to 4, are not activated due to infeasible alignment between supply capacities and demand levels.

Should node 3 be mandated to serve node 4 instead of node 1, there would be no surplus production in the network to bridge the deficit in the demand of node 1. This implies that, in this exceptional case, the optimization procedure is compelled to establish a longer link between nodes 3 and 1 to comply with the supply and demand matching constraint (refer to Eq. (11)). Analogous explanations can be extrapolated to other potential connections in the network.

Thus, the number and dimensions of the production facilities are selected to prioritize the fulfillment of local demand in each subregion.

Lastly, the aggregated hydrogen demands for FCMUs and FCEBs have been considered in Scenario 3, and optimized results have been reported in Fig. 6.

In this scenario, larger electrolyzer sizes are necessitated to ensure the fulfillment of the hydrogen demands for trains and buses across all nine subregions in Sicily. The optimized network manifests a higher

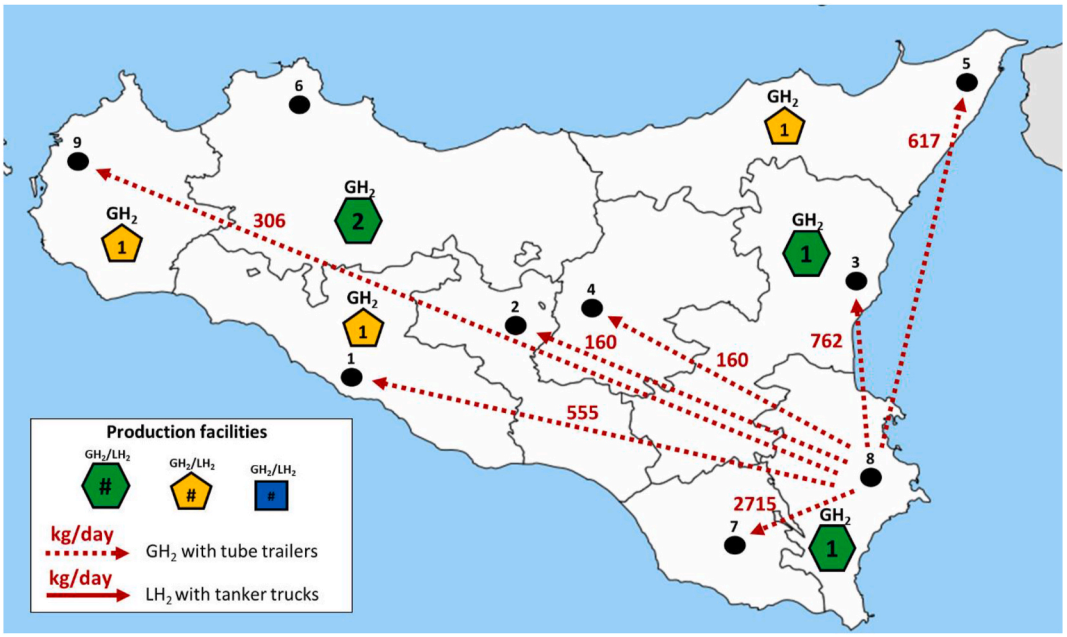

Fig. 6. Optimized HSC for scenario 3, considering FCMUs and FCEBs.

degree of centralization (as elaborated further later), making it markedly different when compared to Scenarios 1 and 2. This primarily stems from the total demand being more than tenfold higher than that of Scenario 1.

Interestingly, one of the Sicilian subregions, specifically subregion 8, emerges as a viable candidate for a hydrogen production hub. It holds the potential to meet the demands of all the other subregions, even when local production facilities are already installed, as it the case of subregions 1 and 3.

Consistent with Scenarios 1 and 2, in Scenario 3, nodes 3, 7, and 8 act as the primary production hubs, producing the majority of the hydrogen that is then conveyed to other subregions. This renders these nodes as ideal locations for establishing hydrogen production hubs capable of catering to most demand points within the region. Moreover, subregions 8 and 3 exhibit a high availability of wind energy, as indicated in Table 1.

Indeed, the more decentralized the HSC becomes, the more demand is being satisfied by local production. The degree of decentralization of within the HSC can be assessed by calculating the portion of the overall demand met by local production, which stands at 80%, 92%, and 87% respectively.

An overview of the HSC costs stemming from the optimization across the three scenarios is reported in Table 13. These data refer to the entire Sicilian HSC. It is noteworthy that, in terms of cost breakdown, the preponderant contribution derives from the capital costs associated with establishing production and refueling facilities. They account for more than 91% of the total costs for each scenario, trailed by the costs incurred in implementing transport modes, which constituted about 4% of the final costs. Nonetheless, the costs avoided for newly constructed wind farms significantly bolster this approach from an economic perspective, thus underpinning the economic sustainability of the entire HSC. As observed, the unit cost of 1 kgH_2 dispensed at the refueling station varies in each scenario, being 9.02 €/kgH_2, 6.34 €/ kgH_2 and 6.32 €/kgH_2, respectively. It decreases when the total demand for the HSC increases. This is explained by the well-established principle of economies of scale, i.e., final unit costs decrease as production volumes increase. Scenarios 2 and 3 exhibit marginally different unit costs since FCEBs demand constitute more than 93% of that in Scenario 3. Scenario 1 exhibits significantly higher values than the others owing to its low level of final hydrogen demand. The Italian gasoline cost, presumed for diesel vehicles, is assumed to be 1.725 €/l or 2.3 €/kg [53].

The optimized results are leverage to undertake an environmental assessment of the established supply chain. Specifically, across the three scenarios, the total amount of avoided CO_2 emissions at the production stage is calculated, as shown in the second row of Table 14. As described in the "Materials and Methods" section, all the energy harnessed for hydrogen production is considered renewable. Thus, the daily avoided emissions can be equated to the amount of emissions that would have been generated if all the energy used for hydrogen production had been supplied by the power grid. This calculation is performed by applying the average emission factor of the Italian power grid. Conversely, for the distribution stage, the environmental analysis is pursued by calculating the total amount of CO_2 emissions generated due to the operation of diesel-fueled trucks. This quantity is determined by multiplying the total count of kilometers traversed by all trucks operative within the network, which is an optimized variable, by the emission factor of their fuel per kilometer. The results in terms of emissions associated with the distribution stage are reported in the first row of Table 14. The average emission factor per traversed km attributable to a diesel truck is equal to 1.12 $kgCO_{2eq}$/km [54], and the amount of avoided emissions from harnessing energy from renewable sources is pegged at 536 $kgCO_{2eq}/kWh$ [46], which aligns with the average emission factor of the Italian power grid.

It is evident that the carbon emissions due to the distribution stage increase with the increase in hydrogen demand. This occurs because more transportation units, i.e., trucks, are deployed within the network to deliver hydrogen to refueling stations. However, this increase is not comparable to the benefit in terms of avoided emissions achieved by exploiting electricity produced from renewable sources (i.e., wind farms), and therefore, not attributable to fossil sources.

Table 13
Overview of the HSC costs for the three optimized scenarios.

	Scenario 1 (FMUs)	Scenario 2 (FCEBs)	Scenario 3 (FCMUs and FCEBs)
Total daily costs [€ /day]	24,043.62	237,902.17	253,905.05
FCC [€]	16,350,458.73	145,155,701.34	153,656,225.60
POC [€ /day]	7441.93	101,039.86	107,647.09
TCC [€]	1,690,650	3,944,850	5,071,950
TOC [€ /day]	125.80	697.42	1300.73
Total costs [€]	18,048,676.45	149,202,288.61	158,837,123.41

Table 14
Environmental analysis for the three optimized scenarios.

	Scenario 1 (FMUs)	Scenario 2 (FCEBs)	Scenario 3 (FCMUs and FCEBs)
Emissions from the distribution stage [$kgCO_{2eq}$ /day]	800.56	1935.23	2358.18
Avoided emissions during the production stage [$kgCO_{2eq}$ /day]	76,367.14	1,035,117.197	1,102,536.30

5. Conclusion

This paper proposed an optimization model to design the HSC for Sicily, the largest Italian island. The model has been built to minimize the total cost of the HSC, from production to refueling, taking into consideration the hydrogen demands for FCMUs and FCEBs. Three scenarios have been identified and optimized; Scenario 1 considers the hydrogen demand for FCMUs in non-electrified Sicilian railways, Scenario 2 for FCEBs bus routes, and Scenario 3 couples the two aforementioned hydrogen demands. The electricity demands for the three scenarios have been attributed to Sicily's numerous wind farms, which are often not in operation due to power grid congestion issues. The key findings of this research can be summarized as follows:

- To foster the sustainable transition to hydrogen-based mobility, the valorization of existing renewable infrastructure can be considered beneficial, suggesting a higher degree of decentralization with the increase in overall hydrogen demand.
- Tube trailers for the transportation of gaseous hydrogen are typically the most cost-effective solution for HSC design, due to the high costs deriving from the construction of expensive liquefaction units at hydrogen production sites.
- Capital costs for building production and refueling facilities contribute to more than 91% of each scenario's overall expenses, while investment and operating costs for transportation modes constitute only 4% of the total expenditures.
- Regarding the environmental analysis, as hydrogen demand rises, so do carbon emissions. However, the benefit in terms of emissions avoided by using electricity from wind (and existing infrastructure) is significantly more impactful.
- Coupling hydrogen demand from FCMUs and FCEBs is reasonable given that they are both characterized by onboard storage tanks with gaseous hydrogen compressed at 350 bars.

An optimization model, such as the one proposed in this study, can serve as a valuable tool for supporting the decision-making process of various stakeholders involved at all stages of the hydrogen supply chain.

By carefully considering the context and setting the boundaries of the analysis, the optimization model can provide the following valuable insights.

Most importantly, the model can guide stakeholders in determining the optimal locations for implementing hydrogen production hubs, taking into account factors such as demand distribution, infrastructure availability, and potential for renewable energy integration. This information can inform decisions on where to invest resources to establish efficient and effective hydrogen production facilities.

Moreover, the optimization model can assist in identifying the most optimal transportation links to connect production hubs with final consumers. By considering factors such as distance, capacity, and operational constraints, the model can guide the establishment of reliable and cost-effective transportation networks within the supply chain.

Finally, the model can assess and optimize the daily hydrogen throughput that each facility should satisfy to minimize disruptions along the supply chain. By considering factors such as production capacities, demand variations, and infrastructure limitations, the model can provide insights into the operating conditions necessary to ensure a smooth and efficient hydrogen supply chain. Overall, the proposed method offers valuable information that can aid stakeholders and policymakers in making strategic decisions, optimizing investments, and ensuring the reliable and sustainable operation of the new hydrogen supply chain.

Future research perspectives could include additional hydrogen demands, for ships, cargo, and ports to further leverage economies of scale. Nonetheless, different hydrogen storage technologies could be considered to absorb yearly demand variability and increase the utilization of non-dispatchable renewable energy sources.

Declaration of competing interest

The authors declare that they have no known competing financial interests or personal relationships that could have appeared to influence the work reported in this paper.

References

[1] Shukla PR, et al., editors. IPCC, 2019: climate Change and Land: an IPCC special report on climate change, desertification, land degradation, sustainable land management, food security, and greenhouse gas fluxes in terrestrial ecosystems; 2019.

[2] CAT Decarbonisation Series. CAT Decarbonisation Series | Freight transport | climate action tracker. 2018.

[3] Ibrahim M, Abdou M, Bakhit M, Mansour P, Dewidar M, Hussein M, et al. Power to gas technology: application and optimization for inland transportation through Nile River. Int J Hydrogen Energy 2022. https://doi.org/10.1016/j.ijhydene.2021.12.143.

[4] European Commission COM. 773 final. A Clean Planet for all A European strategic long-term vision for a prosperous, modern, competitive and climate neutral economy. 2018. Brussels: 2018.

[5] Union European. Committee and the committee of the regions a hydrogen strategy for a climate-neutral Europe. 2020. Brussels.

[6] Italian Ministry for Economy and Finance MEF. PNRR-Next-Generation-Italia_ENG_09022021. 2021.

[7] Ruf Y, Zorn T, Akcayoz De Neve P, Andrae P, Erofeeva S, Garrison F. Andreas Schwilling, Study on the use of fuel cells and hydrogen in the railway environment. 2019. https://doi.org/10.2881/495604.

[8] Coradia iLint - hydrogen fuel cell train, Alstom. https://www.apta.com/wp-content/uploads/Coradia-iLint-%E2%80%93-Hydrogen-Fuel-Cell-Train_James_Varney-1.pdf.

[9] Clean Hydrogen Partnership. Fuel cell electric buses website. https://www.fuelcellbuses.eu/.

[10] Hydrogen Council. Hydrogen scaling up. A sustainable pathway for the global energy transition. 2017.

[11] Trattner A, Klell M, Radner F. Sustainable hydrogen society – vision, findings and development of a hydrogen economy using the example of Austria. Int J Hydrogen Energy 2022;47:2059–79. https://doi.org/10.1016/j.ijhydene.2021.10.166.

[12] International Energy Agency. Global hydrogen review 2021. IEA (2021). Paris: Global Hydrogen Review 2021, IEA; 2021. https://WwwIeaOrg/Reports/Global-Hydrogen-Review-2021.

[13] Cambridge Systematics. Inc., task 8.3: analysis of freight rail electrification in the SCAG region. https://scag.ca.gov/sites/main/files/file-attachments/crgmsais_-_analysis_of_freight_rail_electrification_in_the_scag_region.pdf?1605991886.

[14] Riera Jefferson A, Ricardo M Lima, Knio Omar M. A review of hydrogen production and supply chain modeling and optimization. Int J Hydrogen Energy 2023;48(37):13731–55. https://doi.org/10.1016/j.ijhydene.2022.12.242. ISSN 0360-3199.

[15] Almansoori A, Shah N. Design and operation of a future hydrogen supply chain. Chem Eng Res Des 2006;84:423–38. https://doi.org/10.1205/cherd.05193.

[16] Almansoori A, Shah N. Design and operation of a future hydrogen supply chain: multi-period model. Int J Hydrogen Energy 2009;34:7883–97. https://doi.org/10.1016/j.ijhydene.2009.07.109.

[17] Wickham D, Hawkes A, Jalil-Vega F. Hydrogen supply chain optimisation for the transport sector – focus on hydrogen purity and purification requirements. Appl Energy 2022;305:117740. https://doi.org/10.1016/j.apenergy.2021.117740.

[18] Yoon Ha-Jun, Seo Seung-Kwon, Lee Chul-Jin. Multi-period optimization of hydrogen supply chain utilizing natural gas pipelines and byproduct hydrogen. Renew Sustain Energy Rev 2022;157:112083. https://doi.org/10.1016/j.rser.2022.112083. ISSN 1364-0321.

[19] Ehrenstein M, Galán-Martín Á, Tulus V, Guillén-Gosálbez G. Optimising fuel supply chains within planetary boundaries: a case study of hydrogen for road transport in the UK. Appl Energy 2020;276:115486. https://doi.org/10.1016/j.apenergy.2020.115486.

[20] Almansoori A, Betancourt-Torcat A. Design of optimization model for a hydrogen supply chain under emission constraints - a case study of Germany. Energy 2016;111:414–29. https://doi.org/10.1016/j.energy.2016.05.123.

[21] Seo S-K, Yun D-Y, Lee C-J. Design and optimization of a hydrogen supply chain using a centralized storage model. Appl Energy 2020;262:114452. https://doi.org/10.1016/j.apenergy.2019.114452.

[22] Mah AXY, Ho WS, Hassim MH, et al. Spatial optimization of photovoltaic-based hydrogen-electricity supply chain through an integrated geographical information system and mathematical modeling approach. Clean Technol Environ Policy 2022;24:393–412. https://doi.org/10.1007/s10098-021-02235-4.

[23] Shamsi Hamidreza, Tran Manh-Kien, Akbarpour Shaghayegh, Maroufmashat Azadeh, Fowler Michael. Macro-Level optimization of hydrogen infrastructure and supply chain for zero-emission vehicles on a canadian corridor. J Clean Prod 2021;289(125163). https://doi.org/10.1016/j.jclepro.2020.125163. ISSN 0959-6526.

[24] The hydrogen analysis (H2A) project. https://www.hydrogen.energy.gov/h2a_analysis.html.

[25] Jesus Ochoa Robles, Marialis Giraud Billoud, Catherine Azzaro-Pantel, and Alberto Alfonso Aguilar-Lasserre, Optimal design of a sustainable hydrogen supply chain network: application in an airport ecosystem, ACS Sustainable Chem Eng, 17587-17597, DOI: 10.1021/acssuschemeng.9b02620.

[26] Ibrahim Yasir, Al-Mohannadi Dhabia M. Optimization of low-carbon hydrogen supply chain networks in industrial clusters. Int J Hydrogen Energy 2023;48(36):13325–42. https://doi.org/10.1016/j.ijhydene.2022.12.090. ISSN 0360-3199.

[27] De-León Almaraz S, Azzaro-Pantel C, Montastruc L, Domenech S. Hydrogen supply chain optimization for deployment scenarios in the Midi-Pyrénées region, France. Int J Hydrogen Energy 2014;39:11831–45. https://doi.org/10.1016/j.ijhydene.2014.05.165.

[28] Erdoğan Ahmet, Güray Güler Mehmet. Optimization and analysis of a hydrogen supply chain in terms of cost, CO2 emissions, and risk: the case of Turkey. Int J Hydrogen Energy 2023;48(60):22752–65. https://doi.org/10.1016/j.ijhydene.2023.04.300. ISSN 0360-3199.

[29] Moreno-Benito M, Agnolucci P, Papageorgiou LG. Towards a sustainable hydrogen economy: optimisation-based framework for hydrogen infrastructure development. Comput Chem Eng 2017;102:110–27. https://doi.org/10.1016/j.compchemeng.2016.08.005.

[30] Ochoa Robles Jesus, Azzaro-Pantel Catherine, Aguilar-Lasserre Alberto. Optimization of a hydrogen supply chain network design under demand uncertainty by multi-objective genetic algorithms. Comput Chem Eng 2020;140:106853. https://doi.org/10.1016/j.compchemeng.2020.106853. ISSN 0098-1354.

[31] Victor H. Cantú, Antonin Ponsich, Catherine Azzaro-Pantel, Eduardo Carrera, Capturing spatial, time-wise and technological detail in hydrogen supply chains: a bi-level multi-objective optimization approach. Appl Energy 2023;344:121159. https://doi.org/10.1016/j.apenergy.2023.121159. ISSN 0306-2619.

[32] Hurskainen Markus, Ihonen Jari. Techno-economic feasibility of road transport of hydrogen using liquid organic hydrogen carriers. Int J Hydrogen Energy 2020;45(56):32098–112. https://doi.org/10.1016/j.ijhydene.2020.08.186.

[33] Wilson Rick, Xu Qingyu, Jenkins Jesse D. Minimizing emissions from grid-based hydrogen production in the United States. 2023. https://doi.org/10.1088/1748-9326/acacb5.

[34] Parolin Federico, Colbertaldo Paolo, Campanari Stefano. Development of a multi-modality hydrogen delivery infrastructure: an optimization model for design and operation. Energy Convers Manag 2022;266:115650. https://doi.org/10.1016/j.enconman.2022.115650. ISSN 0196-8904.

[35] Guillén-Gosálbez G, Mele FD, Grossmann IE. A bi-criterion optimization approach for the design and planning of hydrogen supply chains for vehicle use. AIChE J 2010;56:650–67. https://doi.org/10.1002/aic.12024.

[36] Li L, Manier H, Manier M-A. Hydrogen supply chain network design: an optimization-oriented review. Renew Sustain Energy Rev 2019;103:342–60. https://doi.org/10.1016/j.rser.2018.12.060.

[37] Herwartz S, Pagenkopf J, Streuling C. Sector coupling potential of wind-based hydrogen production and fuel cell train operation in regional rail transport in Berlin and Brandenburg. Int J Hydrogen Energy 2021;46:29597–615. https://doi.org/10.1016/j.ijhydene.2020.11.242.

[38] GAMS software GmbH. GAMS Development Corp. n.d. https://www.gams.com/.

[39] IBM. IBM CPLEX Optimizer n.d., https://www.ibm.com/it-it/analytics/cplex-optimizer.

[40] Ursua A, Gandia LM, Sanchis P. Hydrogen production from water electrolysis: current status and future trends. Proc IEEE 2011;100(2). https://doi.org/10.1109/JPROC.2011.2156750.
[41] IRENA. Geopolitics of the energy transformation: the hydrogen factor. https://www.irena.org/publications/2022/Jan/Geopolitics-of-the-Energy-Transformation-Hydrogen; 2022.
[42] Ruth M, Mayyas A, Mann M. Manufacturing competitiveness analysis for PEM and alkaline water electrolysis systems. NREL; 2017.
[43] International Energy Agency IEA. Global hydrogen review: assumptions annex. https://iea.blob.core.windows.net/assets/2ceb17b8-474f-4154-aab5-4d898f735c17/IEAGHRassumptions_final.pdf.
[44] Kecebas A, Kayfeci M, Bayat M. Eletrochemical hydrogen generation. Solar Hydrogen Production, Chapter 9. https://doi.org/10.1016/B978-0-12-814853-2.00009-6.
[45] Navarro RM, Guil R, Fierro JLG. Introduction to hydrogen production. In: Compendium of hydrogen energy. Elsevier; 2015. p. 21–61. https://doi.org/10.1016/B978-1-78242-361-4.00002-9.
[46] Nelabhotla ABT, Pant D, Dinamarca C. Power-to-gas for methanation. Emerging technologies and biological systems for biogas upgrading. Elsevier; 2021. p. 187–221. https://doi.org/10.1016/B978-0-12-822808-1.00008-8.
[47] Clean Hydrogen Partnership. Mission innovation hydrogen valley platform. https://h2v.eu/.
[48] Faye O, Szpunar J, Eduok U. A critical review on the current technologies for the generation, storage, and transportation of hydrogen. Int J Hydrogen Energy 2022; 47:13771–802. https://doi.org/10.1016/j.ijhydene.2022.02.112.
[49] Madovi O, Hoffrichter A, Little N, Foster SN, Isaac R. Feasibility of hydrogen fuel cell technology for railway intercity services: a case study for the Piedmont in North Carolina. Railway Engineering Science 2021;29:258–70. https://doi.org/10.1007/s40534-021-00249-8.
[50] Meneguzzo F, Ciriminna R, Albanese L, Pagliaro M. The remarkable impact of renewable energy generation in Sicily onto electricity price formation in Italy. Energy Sci Eng 2016;4:194–204. https://doi.org/10.1002/ese3.119.
[51] GSE - Gestore dei Servizi Energetici. Il punto sull'eolico (in Italian). https://www.gse.it/documenti_site/Documenti%20GSE/Studi%20e%20scenari/Il%20punto%20sull%27eolico.pdf.
[52] GSE – Gestore dei Servizi Energetici, Atlaimpianti, https://atla.gse.it/atlaimpianti/project/Atlaimpianti_Internet.html.
[53] Autolinee Lumia. Capitolato d'oneri per la fornitura di autobus (in Italian). https://AutolineelumiaCom/Wp-Content/Uploads/2022/02/01_Capitolato-3-02-22.Pdf 2022.
[54] RFI. Rete ferroviaria Italiana. https://WwwRfiIt/It/Rete/La-Rete-Oggi/La_rete_oggi_regione_per_regione/SiciliaHtml.
[55] Circumetnea Catania. Carta dei servizi (in Italian), https://www.circumetnea.it/.
[56] International Council on Clean Transportation. Assessment of hydrogen production costs from electrolysis: united forms and Europe. 2020. Https://Theicct.Org/Sites/Default/Files/Publications/Final_icct2020_assessment_of%20_hydrogen_production_costs%20v2.Pdf.
[57] Parks G, Boyd R, Cornish J, Remick R. NREL, hydrogen station compression, storage, and dispensing technical status and costs. https://www.nrel.gov/docs/fy14osti/58564.pdf.
[58] DOE Hydrogen, Fuel Cells Program Record. Current status of hydrogen liquefaction costs. 2019. https://www.hydrogen.energy.gov/pdfs/19001_hydrogen_liquefaction_costs.pdf.
[59] Ministry of Ecological Transition. Weekly fuel prices. 2022. https://DgsaieMiseGovIt/Prezzi_carburanti_settimanaliPhp?Lang=en_US.
[60] U.S. Environmental Protection Agency US EPA. Emission factors. https://WwwEpaGov/Sites/Default/Files/2018-03/Documents/Emission-Factors_mar_2018_0Pdf; 2018.
[61] U.S. Department of Energy. Hydrogen fueling stations cost. 2020. Https://Www.Hydrogen.Energy.Gov/Pdfs/21002-Hydrogen-Fueling-Station-Cost.Pdf.
[62] Deloitte Monitor. Fueling the future of mobility: fuel cell buses. 2021. https://H2chileCl/Wp-Content/Uploads/2021/11/Fueling-the-Future-of-Mobility-Fuel-CellPdf.
[63] Berger Roland. Study on the use of fuel cells and hydrogen in the railway environment. 2019. https://Shift2railOrg/Wp-Content/Uploads/2019/04/Report-3Pdf.
[64] The International Benchmarking Network IBNET. Water prices compared in 36 EU-cities. 2021. https://WwwIb-NetOrg.
[65] International Renewable Energy Agency (IRENA), Cost of electricity from wind power.